

Nanoindentation of Silicon (100) Studied by Experimental and Finite Element Method

Nurot Panich¹

School of Materials Engineering, Nanyang Technological University, Republic of Singapore, 639798

Rajapark College Management and Technology, Bangkok, Thailand 10310

Email: panich@pmail.ntu.edu.sg

Received 17 December 2003 ; accepted 11 May 2004

Abstract

This study presents the nanoindentation tests of silicon (100) by experimental and simulation techniques. The indentation processes were simulated with the ABAQUS finite element (FE) software programme. The models have the ability to simulate the loading-unloading curves, simulate the development of plastic deformation during indentation and extract intrinsic material property data from the test. Computed load-displacement curves from FE models are compared with the load-displacement curves measured by the experiments. The hardness results obtained from simulation show that they are in good agreement with the measured results.

¹ Assistant Professor, Department of Mechanical Engineering.

1. Introduction

Generally speaking, nanoindentation is one of the simplest ways to measure the mechanical properties of bulk materials or very thin films, particularly the two important properties, hardness and elastic modulus [1-2]. Recently, different numerical techniques have been developed to use in many fields of science and engineering that can be used in indentation problems. Finite element technique is applied for studying the very complex stress-strain field of thin films or bulk materials in a nanoindentation process. Some investigators have studied the indentation process using the numerical approach of finite element method [3-8]. One of the first examples of comparison between FE analysis and experimental results were proposed by Bhattacharya and Nix [9] in which they simulated a sub-micrometer indentation test. So far, the verification of the finite element method could be an effective tool for simulating hardness measurements.

This article presents two-dimensional (2-D) axisymmetric non-linear FE model to simulate the nanoindentation process. The FE results are compared with the experimental results obtained from silicon (100). The results are in the form of load-displacement curves during the loading-unloading process. Owing to the complexity of the phenomena involved in the indentation process, we used the FE program ABAQUS [10] which allows effective modelling of non-linear problems such as the materials properties, the contact between two bodies and the large deformation of the material under the indenter.

2. Experimental Method

Nanoindentation test involves indenting a specimen by a very low load using a high precision instrument, which records the load and displacement continuously. The mechanical properties can be derived from the measured load-displacement curves under loading/unloading through appropriate data analyse. These tests are based on new technologies that allow precise measurement and control of the indenting forces and precise measurement of the indentation depths.

The most popular calibration technique is that of Oliver and Pharr [11] which is based on the elastic solutions of Sneddon [12] for indentation by an axisymmetric body. Since the displacements during unloading are elastic, the relationship between the unloading curve and the elastic modulus of the material being tested can be described by the elastic contact theory. Pharr et al. [13] have shown that the compliance of the contact between any axisymmetric indenter and an elastically isotropic half-space is given by

$$\frac{1}{S} = C_s = \frac{dh}{dP} = \frac{\sqrt{\pi}}{2} \cdot \frac{1}{\sqrt{A}} \cdot \frac{1}{E_r} \quad (1)$$

$$\frac{1}{E_r} = \frac{(1-\nu_s^2)}{E_s} + \frac{(1-\nu_i^2)}{E_i} \quad (2)$$

where S is the experimentally measured stiffness of unloading data, A is the projected area of the contact, C_s is the specimen's compliance, h is the penetration depth and P is the load on the indenter. E_r is the reduced modulus owing to take account of the effects of elastic deformation of indenter (non-rigidity). Reduced modulus is the combined modulus of the indenter and the specimen. E_s , ν_s , E_i and ν_i are the elastic modulus and Poisson's ratio of the specimen and indenter, respectively. Equation (2) has its origins in elastic contact theory and many investigators support that it can apply to any indenter that can be described as a body of revolution of a smooth function. In the usual way we define the hardness of the material, H , to be the mean pressure exerted by the indenter at maximum load,

$$H = \frac{P_{\max}}{A} \quad (3)$$

where P_{\max} is the maximum load applied during the indentation and A is the projected area of contact between the indenter and the specimen. The measurements of indentation modulus and hardness depend on knowing the contact area of the indentations. The expression for the contact area according to a Berkovich indenter is usually estimated by the formula as follows:

$$A(h_c) = 24.5h_c^2 + C_1h_c^1 + C_2h_c^{1/2} + C_3h_c^{1/4} + \dots + C_8h_c^{1/28} \quad (4)$$

where h_c is the contact depth or the specimen displacement and C_1 through C_8 are constants. The lead term describes a perfect Berkovich indenter while the others describe deviations from the Berkovich geometry due to blunting at the tip.

Silicon (100) was chosen for use in this study because of very smooth surface. In addition, such the material was indented by diamond Berkovich indenter in sub-micron or nano-scales and performed to a depth of 300 nm. The experiment is performed using the NanoTest™ [14] from Micro Materials Limited., Wrexham, United Kingdom. The NanoTest™ device measures the movement of a calibrated diamond indenter penetrating into a specimen surface at a controlled loading rate. This device uses a pendulum pivoted on bearings which are essentially frictionless.

3. Finite Element Modelling (FEM)

In the present study, the 2-D axisymmetric case is performed to simulate the elastic-plastic indentation process by the ABAQUS finite element (FE) code [10]. The conical rigid indenter is used in the model in order to define an axisymmetric model. The indenter has a half-angle of 70.3° , and thus has the same projected area-depth function as the standard Berkovich indenter. The specimen is modelled with 7,841 four-node axisymmetric reduced integration elements (CAX4R element type [10]), as shown in Figure 1. In order to study the stress distribution under the indenter when the load applied, a fine mesh is used under the contact area and near the tip of the indenter which the finest mesh element is the square of 20 nm. The mesh is continuously coarser further away from the tip, as shown in Figure 2. The indentation process is simulated both during loading and unloading step. During loading process the simulation is performed to a depth of 500 nm in the y-direction, i.e. the indenter tip penetrates into the specimen; while during unloading process the indenter tip returns to the initial position (0, 0, 0).

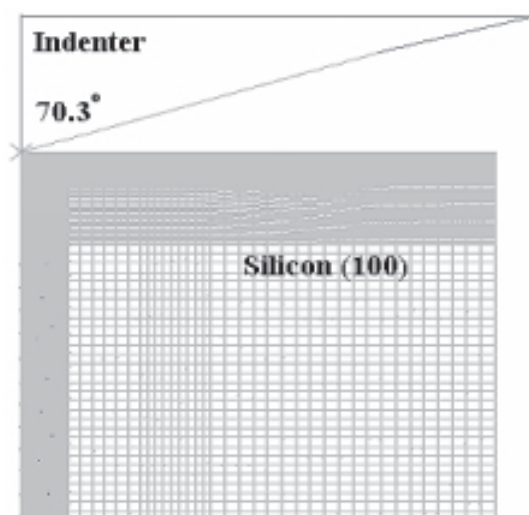


Figure 1. Mesh of the entire specimen with the indenter for 2-D model.

The contact constraint is defined as the master and the slave surfaces. Due to fact that only the master surface can penetrate into the slave surface, the contact direction is then determined with respect to the master surface. The model chooses the indenter as the master surface and sample as the slave surface. The boundary conditions are applied along the original point, centerline and bottom of specimen by fixing the sample at the horizontal axis. The friction between the indenter tip and the specimen surface is assumed to be zero. The nanoindentation model was developed by based on the following assumptions, i.e. there is no strain hardening of the materials used in model and there is the perfectly interfacial bonding between the indenter and the substrate.

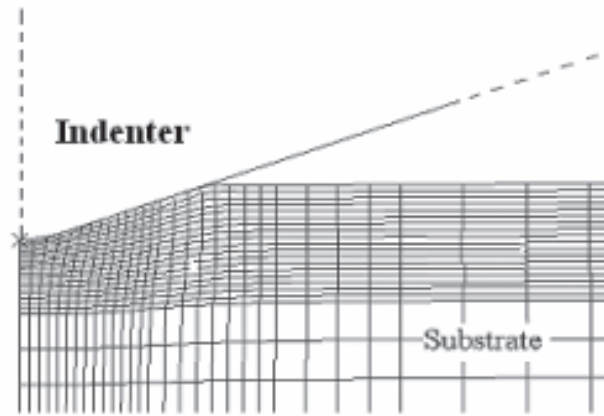


Fig. 2. Details of the mesh in the region near the tip of the indenter.

In the calculation, the elastic deformation occurs in the beginning of the process. The Mises yield criterion is applied in the occurrence of the plastic deformation. The Mises stress equation is given by the expression

$$\sigma_{Mises} = \sqrt{\frac{(\sigma_1 - \sigma_2)^2 + (\sigma_2 - \sigma_3)^2 + (\sigma_3 - \sigma_1)^2}{2}} \quad (5)$$

where σ_1 , σ_2 and σ_3 are the three principle stresses. When the σ_{Mises} reaches the yield strength of material (σ_Y), the specimen starts to deform to the plasticity. Some necessary mechanical properties used in the simulation for silicon (100) are Young's modulus, $E = 130$ GPa; Poisson's ratio, $\nu = 0.28$; and yield strength, $\sigma_Y = 7$ GPa [15].

4. Results and Discussion

Fig. 3 shows the loading curves to compare between the experimental results and the FE calculation. The load-displacement curves measured from various nanoindentation tests demonstrate the repeatability of results from several nanoindentation tests. The FE result shows an excellent trend when compared to the experimental results. From Fig. 3, it obviously shows that the FE model behaves consistently harder than the experimental results slightly until an indentation depth of 200 nm. This may be due to the differences in mesh refinement in the area near the indenter tip and/or the deviation from the deformation of tip indenter during experiment.

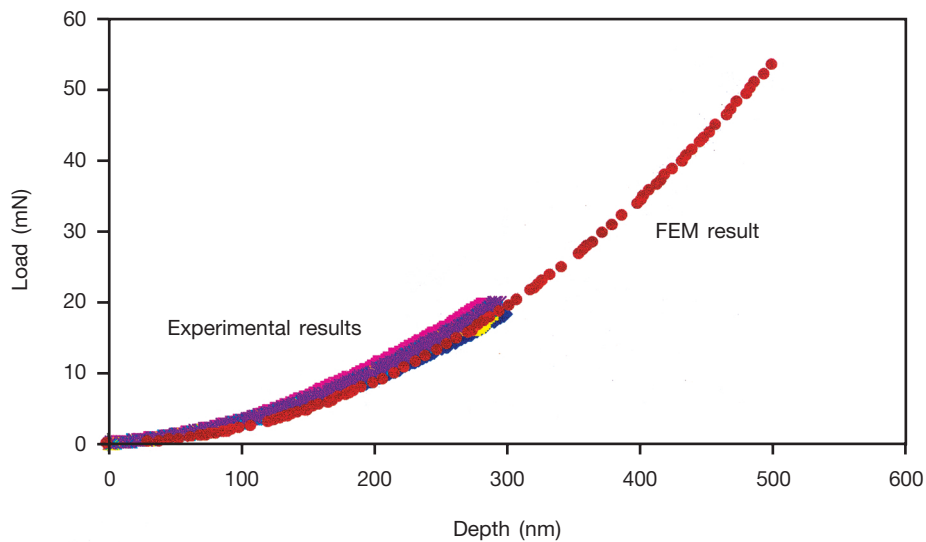


Fig. 3. The load-displacement curves from finite element method with conical indenter and experimental results.

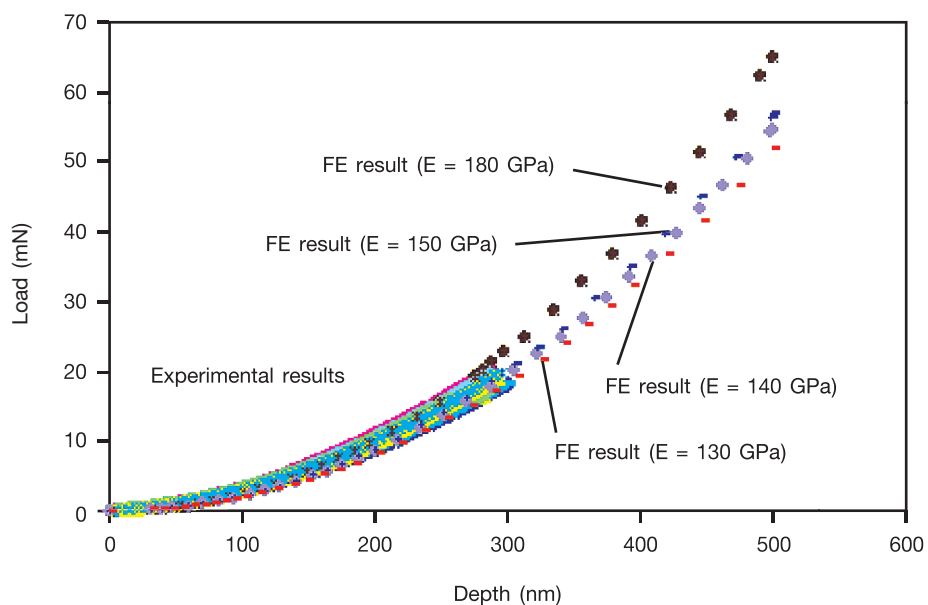


Fig. 4. The load-displacement curves between finite element calculations increased the values of Young's modulus and experimental results.

As the Young's modulus of silicon found in literature was very low for the elastic-plastic model when compared with the measured values, as shown in Table 1. Table 1 has been given elsewhere [N. Panich and Y. Sun 2002, unpublished].

Table 1. Comparison of experimentally measured Young's modulus with value in the literature.

Material	Experiment E (GPa)	Literature		Reference
		E (GPa)	ν	
Silicon (100)	151.8	130	0.28	15

From this result, we have then tried to improve the agreement between the experimental results and model, by increasing the young's modulus of silicon which is based on the measured values. Fig. 4 shows the FE results of increasing the Young's modulus of silicon to 140, 150 and 180 GPa. From the Fig. 4, the best value for the modulus has been found to be about 180 GPa. Fig. 5 depicts the Mises stress contours (plastic deformation) for the 2-D axisymmetric FE model by showing the levels of the stress away from the indenter tip vicinity. The maximum stress magnitudes are in the region under the tip. The maximum stresses computed from Mises stress criterion have values of 7 GPa as shown in the colour bar.

The simulation of the development of plastic deformation in silicon (100) was investigated in order to gain a better understanding of the deformation behaviour in the material as the indentation depth is increased.

Fig. 5 shows the propagation of the plastic deformation zone in silicon (100) material. At small indentation depths, plastic deformation takes place around the indenter tip region, which propagates both vertically and laterally as round shape (Fig. 5 (a)). At larger indentation depths, plastic deformation also propagates both vertically and laterally but the plastic deformation zone is larger than when compared with the case of small indentation depths as shown in Fig. 5 (b).

A further study has been conducted in order to extract the intrinsic mechanical properties using the developed FE model. Fig. 6 shows the load-displacement curves resulted from experiment of silicon (100) together with the prediction from simulation modelling, and the input data from the above analysis (best fit). Since the experimental data were used as the basis of the simulation, such as the yield strength and Poisson's ratio, it is not surprising that there is a good agreement between the simulation and experimental results.

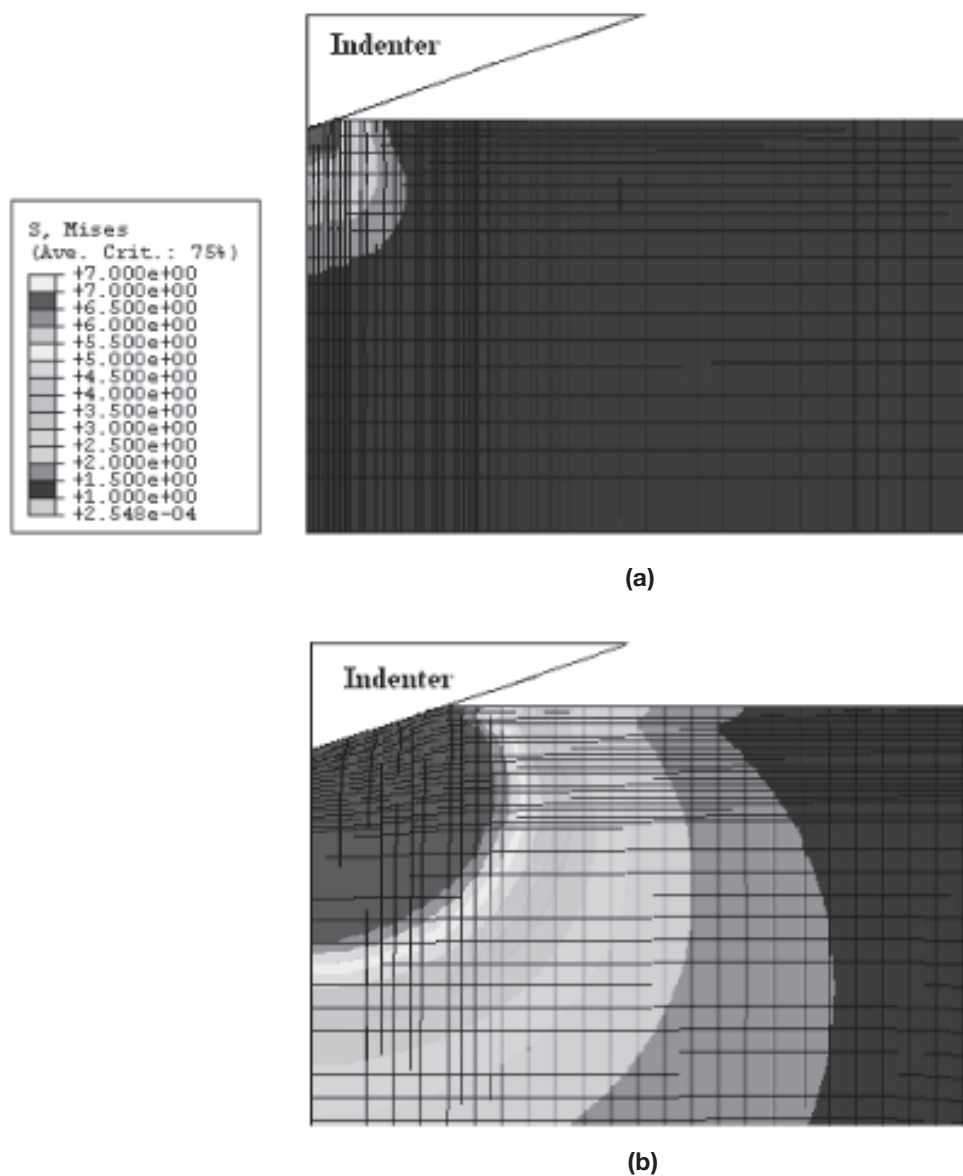


Fig. 5. The Mises stress contours (plastic deformation) for 2-D axisymmetric FE model as the indentation depth is increased.

Fig. 7 shows the comparison of hardness between the experiment and FEM. It is noted that FEM is able to extract intrinsic material properties. From these results, the model has shown the reliability and possibility to apply this model to the single-layer system (thin film system), which will be discussed in a forthcoming publication.

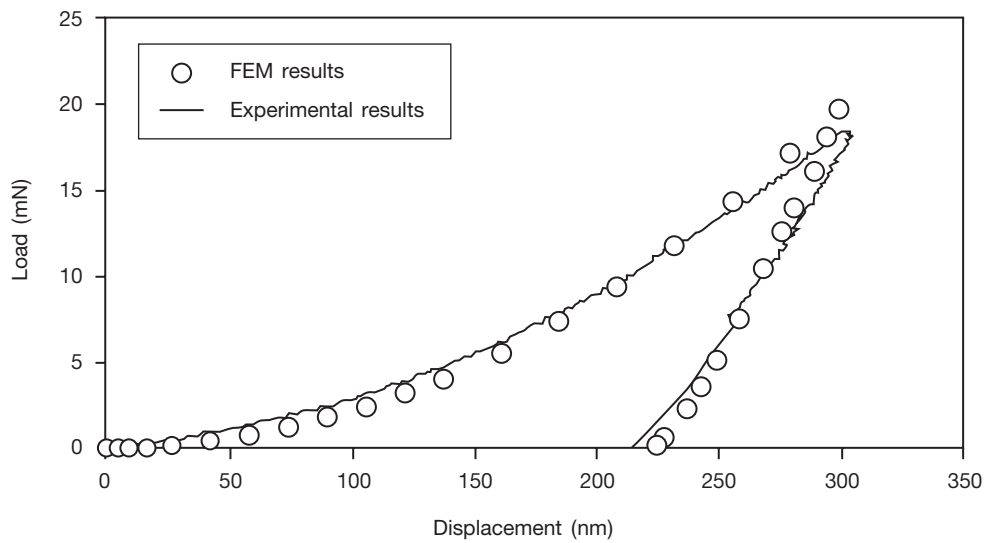


Fig. 6. Comparison of simulated results with experimental data.

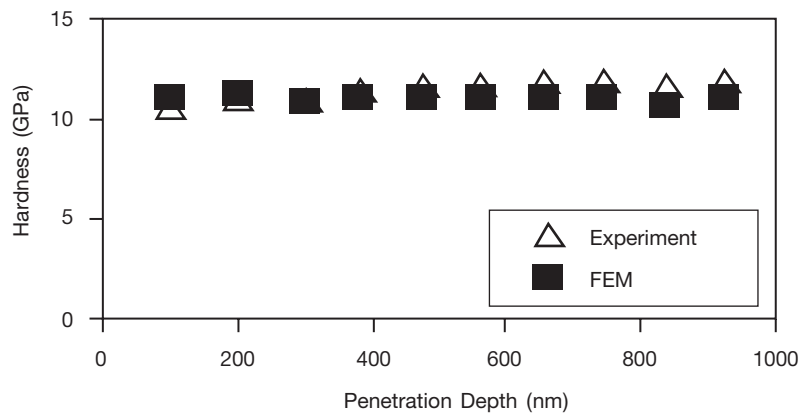


Fig. 7. The comparison of hardness between the experiment and the calculated method.

5. Conclusions

Finite element method is a powerful device to simulate the indentation process at the nano-scale. This study presents 2-D axisymmetric FE model to predict the nanoindentation procedures. The FE results-load-displacement curves compare well with the measured results of silicon (100), even if there is a slight deviation in the loading curves which the deviation relies on the Young's modulus of specimen. Furthermore, in order to extract the intrinsic mechanical properties of silicon sample, the model shows the best fit curve that the value of elastic modulus should be about 180 GPa. The developed model also has been successfully used together with the nanoindentation experiments to extract intrinsic mechanical properties such as hardness for silicon (100).

6. Acknowledgement

The author would like to thank Prof. Dr. Y. Sun (NTU, Singapore) for the technical assistance.

7. References

1. Hay, J. L. and Pharr, G. M., 2002, in *ASM Handbook Volume 8: Mechanical Testing and Evaluation, 10th ed.*, edited by H. Kuhn and D. Medlin (ASM International, Materials Park, OH) pp. 232-243.
2. Pharr, G. M. and Oliver, W. C., 1992, "Measurement of Thin Film Mechanical Properties using Nanoindentation", *MRS Bulletin*, Vol. 7, pp. 28-33.
3. Sun, Y., Bell, T., and Zheng, S., 1995, "Finite Element Analysis of the Critical Ratio of Coating Thickness to Indentation Depth for Coating Property Measurement by Nanoindentation", *Thin Solid Films*, Vol. 258, pp.198-204.
4. Bolshakov, A., Oliver, W. C., and Pharr, G. M., 1996, "Influences of Stress on the Measurement of Mechanical Properties using Nanoindentation: Part II. Finite Element Simulations", *Journal of Material Research*, Vol. 11, pp. 760-768.
5. Lichinchi, M., Lenardi, C., Haupt, J., and Vitali, R., 1998, "Simulation of Berkovich Nanoindentation Experiments on Thin Films using Finite Element Method", *Thin Solid Films*, Vol. 333, pp. 278-286.
6. Vlachos, D. E., Markopoulos, Y. P., and Kostopoulos, V., 2001, "3-D Modeling of Nanoindentation Experiment on a Coating-substrate System", *Computational Mechanics*, Vol. 27, pp. 138-144.
7. Tunvisut, K., Busso, E. P., and O'Dowdy, N. P., 2002, "Determination of the Mechanical Properties of Metallic Thin Films and Substrates from Indentation Tests", *Phil. Mag. A*, Vol. 82, No. 10, pp. 2013-2029.
8. Knapp, J. A., Follstaedt, D. M., Myers, S. M., Barbour, J. C., and Friedmann, T. A., 1999, "Finite-Element Modeling of Nanoindentation", *J. Applied Physics*, Vol. 85, pp. 1460-1474.
9. Bhattacharya, A.K. and Nix, W.D., 1988, *Int. J. Solids Struct.*, Vol. 24, pp. 881.
10. Hibbitt, Karlsson and Sorensen, 2002, Inc., *ABAQUS*, Version 6.3, User's Manual, Pawtucket, RI.
11. Oliver, W. C. and Pharr, G. M., 1992, "An Improved Technique for Determining Hardness

and Elastic Modulus using Load and Displacement Sensing Indentation Experiments”, *Journal of Material Research*, Vol. 7, pp. 1564-1583.

12. Sneddon, I. N., 1965, “The Relation between Load and Penetration in the Axisymmetric Boussinesq Problem for a Punch of Arbitrary Profile”, *Int. J. Engng. Sci.*, Vol. 3, No. 47.

13. Pharr, G. M., Oliver, W. C., and Brotzen, F. R., 1992, “On the Generality of the Relationship between Contact Stiffness, Contact Area, and Elastic Modulus during Indentation”, *Journal of Material Research*, Vol. 7, pp. 613-617.

14. NanoTest™, Micro Materials Limited, Wrexham, United Kingdom.

15. Peterson: Silicon as a Mechanical Material, 1982, *Proc. IEEE*, Vol. 70, No. 5, pp. 420-475.